14th International Particle Accelerator Conference,Venice, Italy JACoW Publishing
ISBN: 978-3-95450-231-8 ISSN: 2673-5490 doi: 10.18429/JACoW-IPAC2023-TUPA062

CYCLOTRON RESONANCE ACCELERATOR FOR ELECTRON BEAMS*

X. Chang†, Y. Jiang, J.L. Hirshfield
Particle Accelerator Research Foundation - PARF, New Haven, CT, USA
M. Fedurin, M. Palmer, W. Stern, Brookhaven National Laboratory, Upton, NY, USA

Abstract

Results from the single-particle equations of motion for electrons traversing an idealized TE-111 mode cavity in an external magnetic field near cyclotron resonance [1] show acceleration rates that substantially exceed the limits for the CARA interaction [2,3]. We have dubbed this new accelerator "eCRA." Here we report on new CST simulation results for realistic cavity designs, finite space-charge beams, transient response, and possible wake fields that essentially confirm the former single-particle idealized solutions. We present a few eCRA simulations for a copper room-temperature TE-111 mode cylindrical cavity. The S-band example shows acceleration of a 4.4 A beam to 3.5 MeV, with an RF wave-particle efficiency of 60%; the 1 GHz example shows acceleration of a 5.5 A beam to 7.2 MeV with an efficiency of 75%; and the 650MHz example show the possibility of achieving a 5.8 A beam with 7.2 MeV energy and 83% efficiency. These results augur well for realization of an eCRA-based x-ray source to replace widely-used Co-60 and Cs-137 gamma sources now in use for sterilization. Many other applications have been identified for MW-class eCRA beams with energies in the range 1-10 MeV [4].

INTRODUCTION

Details of the **e**lectron **C**yclotron **R**esonance **A**ccelerator (eCRA) concept and its underlying theory can be found in [1]. Here we summarize the main features of eCRA. First, we show results based on numerical solutions of the equations of the motion in the fields of a TE-111 mode cylindrical cavity in a dc magnetic field B_o, and then present new results obtained from PIC-code simulations that include beam space-charge effects, transient and wake field effects, and realistic cavity features.

Examples of particle trajectories in an S-band eCRA cavity are shown in Fig. 1. With a peak electric field at the cavity wall of 100 MV/m, the beam final energy for case (a) is 10.13 MeV, while case (b), where the particles are reflected in the cavity, shows the need to exercise care in the choice of eCRA parameters. As yet, no universal algorithm has emerged that can predict conditions for reflections, other than too high a B_o-field.

Results shown in Figs. 1-4 were obtained from solutions of the single-particle equations of motion in the vacuum fields of an idealized TE-111 cylindrical microwave cavity [1]. Acceleration by 10 MeV as shown in Fig. 1(a) occurs in one turn of the orbit. Realistic field distortions from coupling apertures, beam ports, and space charge were not included. Particle-in-cell simulations of the beam dynamics in a realistic cavity are described in the remainder of this paper. These simulations include apertures for beam entry and exit, RF couplers, beam space charge effects, transient cavity filling, and wakefields.

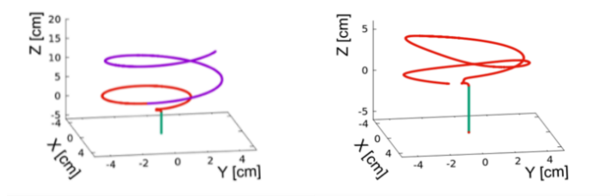

(a) (b)

Figure 1: Particle orbits for two S-band eCRA cavities. (a) Cavity radius R = 6 cm and cavity length L =6.113 cm, magnetic field B_o = 0.914 T, peak E field on wall E_W = 100 MV/m, injection energy of 100 keV (green portion), the beam exits from cavity (violet portion) with final energy of 10.13 MeV. (b): Beam is reflected back (red), R = 7 cm, L =5.84 cm, B_0 = 0.65 T, E_W = 100 MV/m, initial energy = 100 keV.

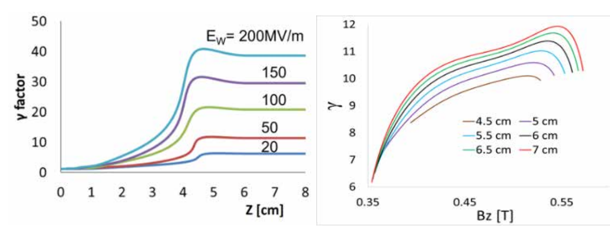

(a) (b)

Figure 2 (a): Final energy factor γ of particles vs. E_W. for an S-band cavity with frequency of 2856 MHz. (b): Final energy factor γ of beam for E_W = 50 MV/m vs. B_Z in S-band cavities with various radius values.

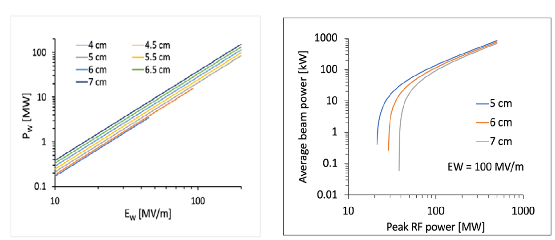

(a) (b)

Figure 3 (a): Peak RF input power to achieve the indicated wall field E_w for S-band eCRA cavities of the indicated radii. (b): Average beam power vs. RF power for S-band cavities of indicated radii, for E_w =100 MV/m

* Work sponsored in part by Brookhaven National Laboratory LDRD 23-060 and Particle Accelerator Research Foundation (PARF).
† xychang6666@gmail.com

ISBN: 978-3-95450-231-8 ISSN: 2673-5490 doi: 10.18429/JACoW-IPAC2023-TUPA062

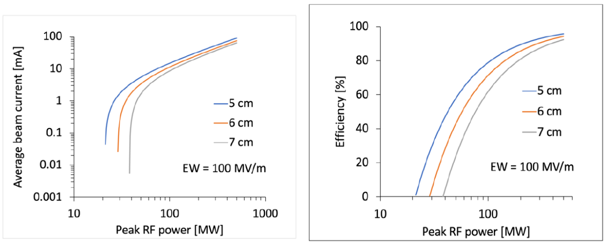

(a) (b)

Figure 4 (a): Average current vs. RF power. E_w =100 MV/m. (b): Efficiency vs. peak RF power for S-band cavities with the three indicated radii, at E_w=100 MV/m.

RESULTS FROM PIC SIMULATIONS

The mechanical design of a S band eCRA cavity is illustrated in Fig. 5. The CST Particle Studio Particle-In-Cell (PIC) solver was used for beam dynamics simulations. Results in Figs. 6-8 are for an S-band eCRA cavity. The cavity has a radius of 6 cm and a length of 6 cm, a coupling coefficient of about 2.5, and a magnetic field of 3600 G, Beam injection energy is 100 keV. These results show that a 2-mm beam as a whole follows a single particle trajectory as in Fig. 1(a).

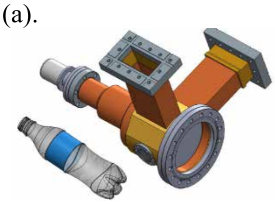

Figure 5: Drawings of the S-band eCRA BNL LDRD Demonstrator cavity. A pint-sized water bottle is added to indicate the size of this S-band eCRA.

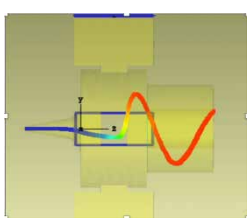

Figure 6: Beam profile at steady-state. The total RF input power is 25 MW, the maximum energy is 3.5 MeV, beam current is 4.4 A, beam power at steady-state is 15.4 MW, and RF efficiency with beam on is 60%. Frequency: 2.856 GHz.

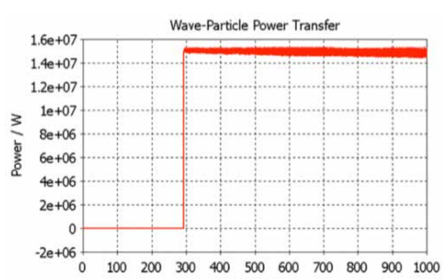

Figure 7: Wave to particle power transfer vs. time. Delay in beam turn-on is the cavity filling time. Frequency: 2.856 GHz.

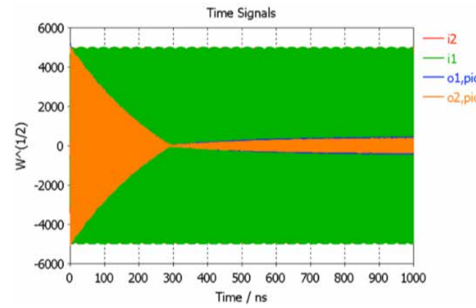

Figure 8: Input signal (i1, i2) and output signal (o1, o2) of the ports of the eCRA cavity with 90 deg phase difference between them. Power in W is half of the square of the signal amplitude. Frequency: 2.856 GHz.

Another example with a lower L-band frequency of 1.019 GHz is shown in Figs 9-11. The cavity radius and cavity length are both 17 cm, and the coupling coefficient is about 4. The injection energy in this case is only 10 keV, the current is 5.5 A, the magnetic field is 2300 G, the total RF input power is 50 MW, the final beam energy is 7.2 MeV, the beam power at steady-state is of 37.5 MW, and the RF efficiency at steady state is 75%.

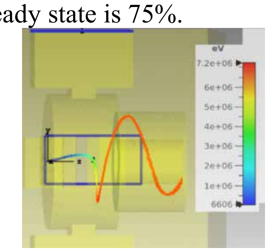

Figure 9: Snapshot of beam profile at the end of the simulation for the 1.019 GHz eCRA cavity example.

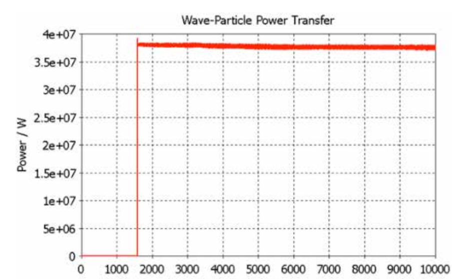

Figure 10: Wave to particle power transfer for the example of the 1.019 GHz eCRA cavity.

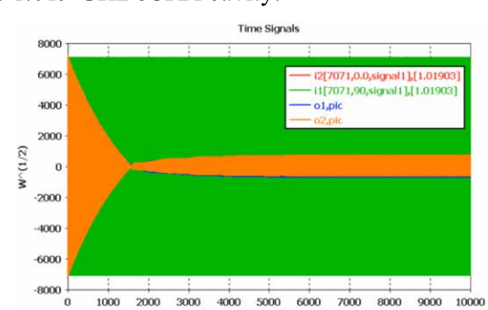

Figure 11: Input signal (i1, i2) and output signal (o1, o2) of an eCRA cavity with RF frequency of 1.019 GHz.

ISBN: 978-3-95450-231-8 ISSN: 2673-5490 doi: 10.18429/JACoW-IPAC2023-TUPA062

Another example with frequency of 650 MHz is shown in Figs 12-14. The cavity radius is 26.15 cm and cavity length is 27 cm. The injection energy in this case is also 10 keV, the current is 5.8 A, the magnetic field is 1500 G, the peak RF input power is 50 MW, the final beam energy is 7.2 MeV, the beam power at steady-state is 41.7 MW, and the RF efficiency at steady state is 83.4%.

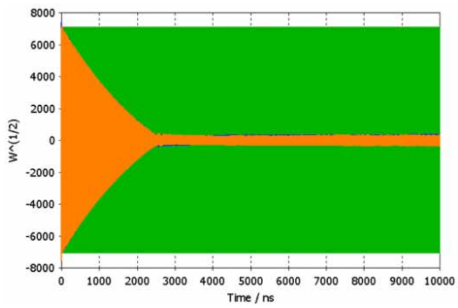

Figure 12: Input signal (i1, i2) and output signal (o1, o2) of a eCRA cavity with RF frequency of 650 MHz.

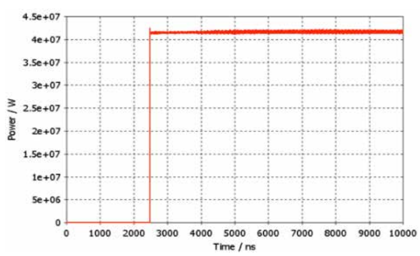

Figure 13: Wave to particle power transfer for the example of the 650 MHz eCRA cavity.

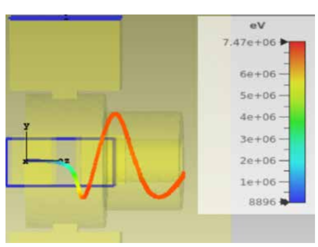

Figure 14: Snapshot of beam profile at the end of the simulation for the 650 MHz eCRA cavity example.

The use of the realistic magnetic field is seen to show negligible influence on beam dynamics.

The simulations also indicate that the beam trajectory remains stable, even with small energy spread, and over a wide magnetic field variation range (~20%). No evidence in these simulations for wake field disruptions is seen, although such disruptions were observed in simulations for cavities with asymmetrical wall features. Stable behavior for the high-current examples shown here may be attributed to the absence of beam bunching.

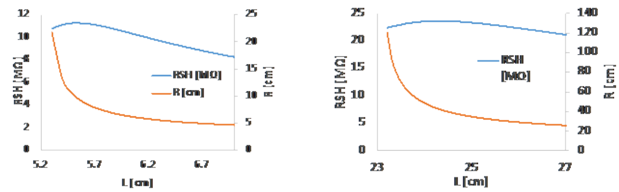

(a) (b)

Figure 15: (a): Shunt impedance vs. cavity length for S-band (2856 MHz). (b): for UHF-band cavity (650 MHz).

Figure 15 is the plot of the shunt impedance as a function of cavity dimensions, where the shunt impedance is defined as $R_{SH} = V^2/P$, and $V = 2E_W R$ is a measure of the energy that could be gained by an electron if in its gyration through the cavity of radius R it remained in phase with the rotating E-field. The power $P = \omega U/Q$ is that necessary to sustain the wall field E_W without the beam. This comparison of shunt impedance at two frequencies shows that a lower frequency cavity is preferred for higher R_{SH} and therefore higher efficiency, as well as lower magnetic field. The three examples also demonstrate that a lower frequency cavity is preferred for achieving higher beam energy and higher efficiency, as the simulations above show.

CONCLUSIONS

- Simulations for the eCRA acceleration mechanism using CST-PIC Solver confirm published results that are based on single-particle theory [1].
- Use of a realistic B-field profile and a realistic cavity geometry do not impair the eCRA mechanism.
- Simulation runs out to 10 μsec show no evidence of beam instability for cavities that avoid asymmetrical wall features.
- Use of a thin Beryllium foil or Aluminum foil at the beam exit channel is a viable solution to contain the RF cavity fields and to allow passage of the beam.
- Future eCRA designs should be at a frequency lower than 2856 MHz to capitalize on higher shunt impedance.
- Achievement of MW-class average beam powers, as desired for various applications, will require development of higher average-power RF sources having the requisite peak power output. Development of MW-class average-power RF sources remains an issue for all RF-based accelerator technologies.
- Existing RF sources are adequate for eCRA-based x-ray sources with up to ~200 kW average power. This will enable replacement of radioactive Co-60 and Cs-137 gamma sources in many applications.

ISBN: 978-3-95450-231-8 ISSN: 2673-5490 doi: 10.18429/JACoW-IPAC2023-TUPA062

REFERENCES

[1] S.V. Shchelkunov, X. Chang, J.L. Hirshfield, "Compact cyclotron resonance high-power accelerator for electrons," *Phys. Rev. Accel. Beams,* vol. 25, p. 021301, 2022.

[2] M.A, LaPointe, R.B. Yoder, C.B. Wang, A.K. Ganguly, J.L. Hirshfield, "Experimental demonstration of high-efficiency cyclotron autoresonace acceleration," *Phys. Rev. Lett*. Vol. **76**, 2718 (1996).

[3] J.L. Hirshfield, C.B. Wang, "Energy limit in cyclotron autoresonance acceleration," Phys. Rev. E **51**,2446 (1995).

[4] Basic research needs workshop on compact accelerators for security and medicine: Tools for the 21st century, 2019, Michael Fazio, chair; Office of Science, US Department of Energy.